First-principles study of the cubic perovskites BiMO_3 (M=Al, Ga, In, and Sc)

Hai Wang,[1] Biao Wang,[1,2] Qingkun Li,[1] Zhenye Zhu,[1] Rui Wang,[3] and C. H. Woo[4]
[1]*School of Astronautics, Harbin Institute of Technology, Harbin 150001, China*
[2]*School of Physics and Engineering, Sun Yat-sen University, Guangzhou 510275, China*
[3]*Department of Applied Chemistry, Harbin Institute of Technology, Harbin 150001, China*
[4]*Department of Electronic and Information Engineering, The Hong Kong Polytechnic University, Hong Kong SAR, China*
(Received 12 September 2006; revised manuscript received 25 March 2007; published 15 June 2007)

We systematically investigated the structure, electronic properties, zone-center phonon modes, and structure instability of four cubic perovskite BiMO_3 compounds, with three of the M ions being IIIB metals (Al, Ga, and In) and one IIIA transition-metal Sc, using first-principles density-functional calculations. Optimized lattice parameters, bulk moduli, band structures, densities of states, as well as charge density distributions are calculated and compared with the available theoretical data. Our results are in good agreement with those previously reported in the literature. All the BiMO_3 oxides considered in the present work are semiconductors with an indirect band gap between the occupied O $2p$ and unoccupied Bi $6p$ states varying between 0.17 and 1.57 eV. Their electronic properties are determined mainly by Bi–O bonding, which, in turn, depends on the M–O bonding. Ferroelectric properties of these oxides come from the $6s^2$ lone pair on the A-site Bi ion and is similarly affected by the M ions through their influence on the Bi–O bonding, as suggested by our calculations of density of state, Born effective charge, and soft modes. The existence of soft modes and eight [111] minima suggests that the phase transition in $BiAlO_3$ has a mixed displacive and order-disorder character. There is evidence that ferroelectricity is absent in $BiGaO_3$. Our investigation suggests that the BiMO_3 oxides or their modified versions are promising ferroelectric, piezoelectric, multiferroic, and photocatalytic materials.

DOI: 10.1103/PhysRevB.75.245209 PACS number(s): 71.15.Ap

I. INTRODUCTION

BiMO_3 compounds, with nonmagnetic elements M, have traditionally been used in the modification of Pb-based piezoelectric materials. Its solid solutions with $PbTiO_3$, for example, are extensively used because they can preserve the high piezoelectric activity up to relatively high temperature and reduce the amount of lead.[1–7] First-principles calculations of piezoelectric alloys xBiScO_3-$(1-x)$$PbTiO_3$ (Ref. 8) suggested that the large structural distortions and polarizations, at the morphotropic phase boundary, come from the hybridization between Bi/Pb $6p$ and O $2p$ orbitals, a mechanism that is enhanced upon the substitution of Pb by Bi. It is reasonable, therefore, to expect that Bi-based compounds would be excellent lead-free piezoelectric materials because they are nontoxic and also have $6s^2$ lone pairs,[9,10] which is the cause of the large ferroelectric polarizations in Pb-based compounds.

To fulfill the requirement of ferroelectricity, BiMO_3 compounds should have a noncentrosymmetric structure (see, e.g., $BiMnO_3$).[11,12] Recently, Baettig *et al.* predicted that bismuth aluminate ($BiAlO_3$) and bismuth gallate ($BiGaO_3$) oxides with perovskite structure were high-performance ferroelectrics and piezoelectrics,[13] in which the large polarization and piezoelectric response are results of the stereochemical activity of the Bi lone pair. It was shown that $BiAlO_3$ shares the antiferroelectric $PbZrO_3$ structure under space group $R3c$, while $BiGaO_3$ has a *tetragonal* perovskite structure, but with stronger distortion and improved ferroelectric properties than that of $PbTiO_3$. Furthermore, the Bi$(Al,Ga)O_3$ systems were proposed as a replacement for the widely used lead-based piezoelectric material [$Pb(Zr,Ti)O_3$ (PZT)], that will avoid the environmental toxicity problems of lead-based compounds.

Experimentally, four BiMO_3 (M=Al, Ga, In, and Sc) compounds have been synthesized by means of high-pressure high-temperature techniques.[14–16] They exhibit many interesting properties with distinct structures at room temperature. $BiAlO_3$ crystallizes in a noncentrosymmetric $R3c$ structure (consistent with the prediction[13]), while $BiGaO_3$ has a centrosymmetric pyroxene-type structure under *orthorhombic* space group *Pcca* rather than the expected tetragonal phase.[14] $BiInO_3$ compound possesses the $GdFeO_3$-type perovskite structure with a polar space group $Pna2_1$. Its second-harmonic generation signal is about 120–140 times that of quartz.[15] $BiScO_3$ is centrosymmetric and has a $BiMnO_3$-type perovskite structure under space group $C2/c$.[16] We note that the four BiMO_3 compounds are unstable: both $BiAlO_3$ and $BiGaO_3$ decompose without phase transition when heated above 820 K as well as $BiInO_3$ above 873 K at ambient pressure.[14,15] In addition, BiMO_3 compounds, where M is magnetic, i.e., M=Mn, Fe, etc., have recently received a lot of attention as multiferroics.[17–20] Finally, BiMO_3 where M is nonmagnetic may be used as model systems to study the origin of ferroelectricity in Bi-based multiferroics, there being no additional complication of magnetic behavior.[13]

First-principles density-functional theory has been successfully applied to investigate ferroelectricity in perovskite oxides including bulk,[21,22] thin films,[23] and superlattices.[24] Cohen first explored the origin of ferroelectricity[25] in bulk materials $BaTiO_3$ and $PbTiO_3$ using the potential energy surface (PES) of the soft mode. Subsequent detailed investigations[26,27] on cubic titanates $ATiO_3$ (A=Ca, Sr, Ba, and Pb) reported that the ferroelectricity came from Ti, and the Ti-O hybridization is essential for it. Recently, Ghita *et al.*[28] redefined the A-site and B-site and AB-site driven ferroelectric according to the PESs of the A- and B-site ions in the

cubic phase, which was usually determined by the tolerance factor, and produced a better understanding of the piezoelectricity of PZT. The hypothetical cubic structure, therefore, is a good prototype for the instigation of ferroelectricity in the ABO_3 oxides (see Refs. 21 and 25–28). Although ferroelectricity had been theoretically predicted in both $BiAlO_3$ and $BiGaO_3$, it was subsequently found to be absent in the latter. The tolerance factor t, an extensively used criterion of structural instability, was found to be unable to describe their ground-state structure.[13] Our previous work also showed a substantial difference between the electronic structures of $BiAlO_3$ and $BiGaO_3$.[29] However, the nature of ferroelectricity and the driving force of the phase transition in BiMO_3 remain unclear.

In this work, we report a systematic study of the structure, electronic properties, zone-center phonon modes, and structural instability of three IIIB-group metals, Al, Ga, and In, and one IIIA transition metal, Sc, in BiMO_3 using first-principles density-functional calculations. The dependence on M of physical parameters such as lattice structure, bulk modulus, band structure, density of state, and electron density distribution is considered. The nature of ferroelectricity in BiMO_3 was investigated and discussed.

II. COMPUTATIONAL METHOD

The considered BiMO_3 are assumed to have ideal cubic perovskite structure (space group $Pm\bar{3}m$), with atomic positions in the primitive cell defined by (M): 1a (0,0,0), (Bi): 1b (0.5,0.5,0.5), and (O): 3d (0.5,0,0). The equilibrium structural parameters and electronic properties were calculated using the WIEN2K package, which is an implementation of the hybrid full potential linear augmented plane wave plus local orbitals (LAPW+lo) method within the density-functional theory.[30] The electronic configurations are taken to be Ne $3s^2 3p^1$ for Al, Ar $3d^{10} 4s^2 4p^1$ for Ga, Kr $4d^{10} 5s^2 5p^1$ for In, Ar $3d^1 4s^2$ for Sc, Xe $4f^{14} 5d^{10} 6s^2 6p^3$ for Bi, and He $2s^2 2p^4$ for O. Here, the noble gas cores are distinguished from the subshells of valence electrons. We use local density approximation[31] (LDA) and/or Perdew-Burke-Ernzerhof generalized gradient approximation[32] (GGA) for the exchange correlation potentials. Relativistic effects are taken into account within the scalar-relativistic approximation. The atomic sphere radii R_{MT} we used are 2.4, 1.6, 1.7, 1.7, 1.8, and 2.0 for Bi, O, Al, Ga, Sc, and In, respectively. We expand the basis function up to $R_{MT}K_{max}=10$, where K_{max} is the largest reciprocal vector used in the LAPW basis set. The k-point sampling in the Brillouin zone is conducted with a $10\times10\times10$ mesh. The self-consistent calculations are carried out with a total energy convergence tolerance of less than 0.1 mRy.

The zone-center phonon modes, dielectric properties, and PESs were calculated using the QUANTUM-ESPRESSO package[33] within density-functional theory[34,35] and density-functional perturbation theory[36] (DFPT) based on a plane-wave basis set and pseudopotentials. We use the norm-conserving pseudopotential (NCPP) with the same electronic configuration. A kinetic energy cutoff of 80 Ry is used and the augmentation charges are expanded up to 240 Ry. Integrals over the Brillouin zone are performed using a Monkhorst-Pack with a $6\times6\times6$ k-point mesh. All calculations are performed using fully optimized structure.

TABLE I. Calculated lattice parameters (Å) and bulk moduli B_0 and its pressure derivative B_0' (GPa) of four cubic BiMO_3.

	Lattice constant	B_0	B_0'
$BiAlO_3$	3.723[a]	218.5	5.15
	3.802[b]	188.5	4.27
	3.715[c]	218.9	4.36
	3.750[d]		
$BiGaO_3$	3.818[a]	206.6	4.67
	3.905[b]	178.6	3.91
	3.821[c]	208.8	4.57
	3.830[d]		
$BiInO_3$	4.193[b]	134.3	5.31
	4.111[c]	158.4	4.15
$BiScO_3$	4.084[b]	134.7	3.63
	3.974[c]	178.5	4.42

[a]LAPW-LDA, Murnaghan equation of state (this work).
[b]LAPW-GGA, Murnaghan equation of state (this work).
[c]NCPP-LDA, second order Birch-Murnaghan equation of state (this work).
[d]NCPP-LDA, Ref. 13.

III. RESULTS AND DISCUSSION

A. Structure

The lattice constants and bulk moduli are calculated by fitting energy volume data to Murnaghan's equation of state.[37] The results are summarized in Table I. It is seen that for $BiAlO_3$ and $BiGaO_3$, the calculated GGA lattice constants are larger than the LDA values. Our LDA results agree well with previous reports for $BiAlO_3$ and $BiGaO_3$.[13] Here, we note that experimental data for the lattice constants of the four cubic BiMO_3 compounds are not available. $BiInO_3$ crystallizes in an orthorhombically distorted $GdFeO_3$-type structure with $a\approx\sqrt{2}a_p$, $b\approx2a_p$, and $c\approx\sqrt{2}a_p$, where a_p is the parameter of the cubic perovskite subcell. The equilibrium lattice constant a_p we obtained is 4.193 Å (GGA). It follows that the lattice constants in $GdFeO_3$-type structure are $a=c\approx\sqrt{2}a_p=5.929$ Å and $b\approx2a_p=8.386$ Å, which agree well with the experimental values[15] of 5.955 and 8.836 Å, respectively. In general, GGA gives better geometrical parameters but usually overestimates the lattice constants and underestimates the bulk moduli.[38] Going from $BiAlO_3$ to $BiInO_3$, the lattice constants increase while bulk moduli decrease, with those of $BiAlO_3$ and $BiGaO_3$ higher than those of $BiInO_3$ and $BiScO_3$. This trend correlates with changes in the lattice constants. We note that two approximations (LDA and GGA) do not affect the trend. The bulk modulus and lattice constant of $BiScO_3$ are between those of $BiGaO_3$ and $BiInO_3$. In addition, the results from full

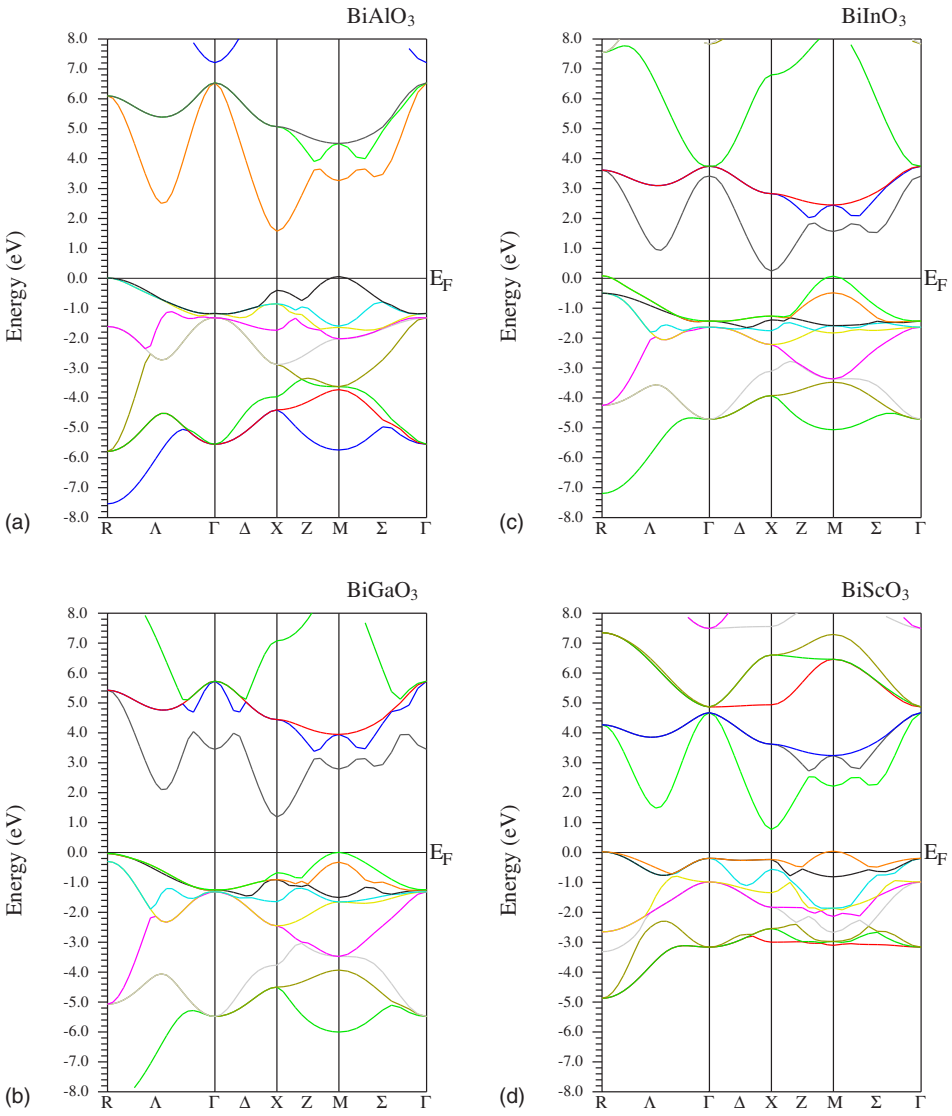

FIG. 1. (Color online) Band structures of four cubic BiMO_3. The Fermi level corresponds to 0.0 eV. All the BiMO_3 are semiconductors with a band gap from 0.17 to 1.57 eV, which is determined by the occupied O $2p$ and unoccupied Bi $6p$ states.

potential linear augmented plane wave agree well with those from norm-conserving pseudopotential within LDA.

B. Electronic properties

1. Band structure

The band structures of the four BiMO_3 compounds along the high-symmetry directions in the Brillouin zone are shown in Fig. 1, where similarities in the energy bands are evident. In the following, the results are discussed using $BiAlO_3$ as an example. The lower bands, which are not shown in Fig. 1, contain Bi $6s$ and O $2s$ states located at −9.8 and −16.5 eV below the Fermi level, respectively. The upper valence band (VB) with a width of about 7.5 eV is mainly derived from the O $2p$ orbitals, with some admixture of the Bi and Al sp states. The top of the valence band of $BiAlO_3$ is composed of O $2p$ orbitals and is located at the M point, while the VB maximum at the R point is about 0.08 eV lower than M. The bottom of the conduction band is located at the X point and is entirely made up of Bi $6p$ states. Thus, the indirect gap between M and X is 1.57 eV, and the direct gap at X is 2.07 eV.

For $BiAlO_3$, the nine occupied bands at the Γ point consist of three triply degenerate levels (Γ_{15}, Γ_{25}, and Γ_{15}) with energies of −5.57, −1.33, and −1.17 eV below the Fermi level, respectively. The splitting of the levels ($\Gamma_{15}-\Gamma_{25}$) is due to crystal field effects and electrostatic interaction between the O $2p$ orbitals. In the conduction band, the triply (Γ'_{25}, +6.55 eV) degenerate levels are from the Bi $6p$ orbitals. These features of the band structure are summarized in Table II. Note that there are no experimental data available for comparison.

Compared to $BiAlO_3$, the band structure of $BiGaO_3$ shows a slightly larger dispersion. For example, the VB bandwidth in $BiGaO_3$ is about 0.71 eV larger. This means that Ga–O bond is more covalent than that between aluminum and oxygen. Another difference is that the band gap, which remains indirect in $BiGaO_3$, is about 0.23 eV smaller than that of $BiAlO_3$. In the case of $BiGaO_3$, the splittings of the bands ($\Gamma_{15}-\Gamma_{25}$) and ($\Gamma_{25}-\Gamma_{15}$) are about 4.26 and 0.11 eV, respectively.

The band structures for $BiInO_3$ and $BiScO_3$ perovskite oxides are also presented in Fig. 1. Their band-structure parameters are listed in Table II. The VBs of $BiInO_3$ and

TABLE II. Calculated values for the bandwidths, valence band splitting at Γ, and band gap (in eV) of BiMO_3.

Parameters	$BiAlO_3$	$BiGaO_3$	$BiInO_3$	$BiScO_3$
Valence band	7.50	8.21	7.12	4.85
Γ_{15}	−5.57	−5.33	−4.66	−3.33
Γ_{25}	−1.33	−1.07	−1.70	−1.00
Γ_{15}	−1.17	−1.18	−1.47	−0.30
$\lvert\Gamma_{15}$-$\Gamma_{25}\rvert$	4.24	4.26	2.96	2.33
$\lvert\Gamma_{25}$-$\Gamma_{15}\rvert$	0.16	0.11	0.23	0.70
Conduction band	6.52	>6.71	>7.83	3.57
	Band gap			
Direct (*X*)	2.07	2.00	1.50	1.16
Indirect (*M*-*X*)	1.57	1.34	0.17	0.83

$BiScO_3$ mainly consist of the occupied oxygen 2*p* bands and partially occupied *M*(In,Sc) *s*,*p*,*d* states. The band structure of $BiScO_3$ obtained agrees well with that previously reported,[8] which is only available along Γ-*X*. The electronic states near the Fermi level originate mainly from O 2*p* states for both oxides. For $BiInO_3$ and $BiScO_3$, the Bi 6*p* states are also dominant in the conduction bands. In the case of $BiInO_3$, the splittings of the bands ($\Gamma_{15}-\Gamma_{25}$) and ($\Gamma_{25}-\Gamma_{15}$) are about 2.96 and 0.23 eV. For $BiScO_3$, these values are about 2.33 and 0.70 eV, i.e., smaller than for $BiAlO_3$ and $BiGaO_3$, respectively. We note that all the cubic BiMO_3 compounds considered here are semiconductors with an indirect band gap in the range between 0.17 and 1.57 eV, which is determined by the occupied O 2*p* and unoccupied *A*-site Bi 6*p* states.

2. Densities of states

The density of states (DOS) was obtained using a modified tetrahedron method.[39] The calculated total density of states (TDOS) and partial densities of states (PDOS) for BiMO_3 are shown in Fig. 2. It can be seen that the TDOS profiles have many peaks that are mostly from the 6*p* states of Bi ion in the conduction bands and 2*p* states of O in the valence bands. For example, in $BiAlO_3$, the valence band originates predominantly from O 2*p* states, which is consistent with $BiAlO_3$, which is a formal *sp* system with aluminum in the 3+ oxidation state. There is also strong hybridization between Al-O due to the same 2*s*2*p* electronic configurations. Both bismuth and aluminum ions also have a small contribution to the valence band. More details can be found in our previous report.[29] A very flat O 2*p*-like band (along Γ-*X*-*M*-Γ, see Fig. 1) is responsible for the highest of them placed at about −1.0 eV. Therefore, the DOS peak at this energy may be attributed to quasiflat bands originating primarily from O 2*p* states.

An equal valence band (or conduction band) width and/or peak value indicate obvious hybridizations between M-O as well as Bi-O. This suggests the presence of covalent bonding, which is important for ferroelectricity. In the region of the valence band, the width of the PDOS of Bi is clearly narrower than that of *M* and O (except in $BiScO_3$). The number of peaks is also less than those for *M*. This indicates that the hybridization of *M*−O is stronger than that for Bi-O. Comparing $BiScO_3$ with other BiMO_3 compounds, we note that the large nonlocal character of the *s* and *p* electrons of *M* (Al, Ga, and In) can effectively widen the valence band. In the case of the conduction band, the peaks are mainly formed from the Bi 6*p* and O 2*p* states. We note that there is little contribution from Al to the conduction band of $BiAlO_3$ in the range of 0–8 eV, in contrast to the contributions from the *M* ions in other BiMO_3 compounds. The lower part of the conduction band of $BiGaO_3$ and $BiInO_3$ ($BiScO_3$) is occupied by the 6*p* state of Bi, while the upper part is mainly occupied by the *s*,*p*(*d*) states of M. These *s*,*p* electrons of Ga and In as well as the *d* electrons of Sc force the Bi 6*p* state to move toward the Fermi level (shown in $BiGaO_3$, $BiInO_3$, and $BiScO_3$). This fact leads to the reduction of the band gap (especially in $BiInO_3$) that is determined by Bi 6*p* and O 2*p* states. In contrast, the band gap of $PbTiO_3$ ($PbZrO_3$), containing another lone pair ion Pb^{3+}, in which the electronic properties and ferroelectric instabilities are mainly characterized by Ti-O and Pb-O hybridizations,[8] is determined by the occupied O 2*p* and unoccupied *B*-site Ti 3*d* (Zr 4*d*) states rather than those associated with Pb-O.

In $BiInO_3$, the Bi 6*s* peak is −10.3 eV below the Fermi level and is shifted by about 0.5 eV relative to that of $BiAlO_3$ (not observable in Fig. 2). In BiMO_3 where *M* are *sp* metals, the strong hybridization occurs between O 2*p* and Al (Ga,In) *p*. When *M* is a transition metal with *d* electrons, it occurs between the O 2*p* and Sc *d*. The transition metal Sc substantially narrows the bandwidths of VBs. While the Bi 6*s* electrons have notable contributions to the top of the valence band in $BiAlO_3$ and $BiGaO_3$, little similar contributions exist in the cases of $BiInO_3$ and $BiScO_3$. In addition, the *d* electrons of Ga, In, and Sc are the major components at the top of the valence band relative to the other *sp* electrons of *M* ions. The difference in the DOS of the four BiMO_3 comes from the difference in the *M* ions, which determines the profiles of the DOS of O ions. Considering the crystal structure of four BiMO_3 compounds at room temperature, it may seem reasonable to expect that the *M* ions play a key role in the structural instability.

3. Charge density

The main contribution to the TDOS at the Fermi level $N_{tot}(E_F)$ in all four oxides originates from the O 2*p* states. To illustrate the bonding picture in these systems, we plot the charge density maps of (110) plane for BiMO_3 in Fig. 3. The $N_{tot}(E_F)$ changes are attributed to the *s*,*p*(*d*) states of *M* as discussed in the foregoing. It can be seen that the hybridization between *M* and O is stronger than that between Bi and O. Although Al^{3+} ions only have 2*s*2*p* electrons, hybridization with O 2*p* states is also observed. Due to the presence of 3*d* electrons, Sc^{3+} ions with 3*s*3*p* electrons exhibit a stronger hybridization with O ions than other *M*−O systems, resulting in a narrow valence band in $BiScO_3$ (Fig. 2). We note that the 4*s*4*p*4*d* electrons in $BiInO_3$ play a smaller role in the hybridization with O 2*p* states than the 3*s*3*p*3*d* ones in $BiScO_3$. The order of hybridization of *M*−O, listed in in-

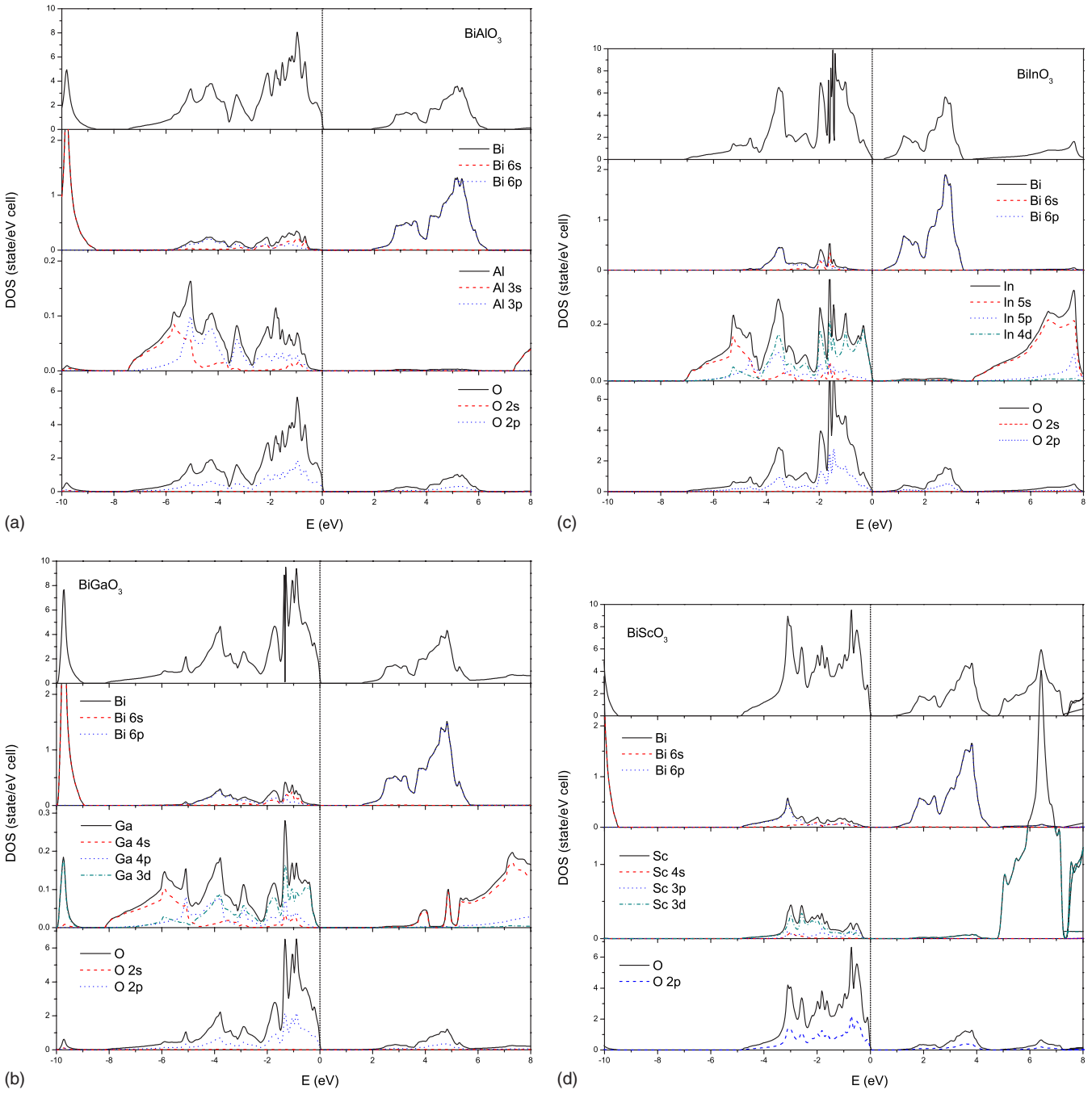

FIG. 2. (Color online) Total and partial DOSs of four cubic BiMO_3.

creasing order, is Al-O, Ga-O, In-O, and Sc-O.

Based on the foregoing results, it is clear that the Bi-O hybridization controls electronic properties listed in Table II, such as band gap. On the other hand, the $M-$O bonding governs the details of Bi-O hybridization shown in Fig. 2. We note that the choice of LDA or GGA does not influence our results. The electronic properties of BiMO_3 in the noncubic structure, such as rhombohedral $BiAlO_3$ (our calculation) and tetragonal $BiInO_3$ (Ref. 8, Fig. 1), are also determined by Bi-O states. Thus, it is interesting that through a proper choice of the M ions, Bi($M1$, $M2$, …)O_3 oxides may be designed to possess desirable electronic properties.

C. Zone-center phonon modes and dielectric properties

1. Born effective charges and dielectric properties

It is well known that anomalously large Born effective charges (BEC) Z^* of atoms are a general feature of perovskite compounds such as titanate, zirconate, and niobate,[40] which are associated with their excellent ferroelectric and piezoelectric properties. Table III shows the calculated Born effective charges and dielectric constants of the four cubic BiMO_3 compounds. For $BiAlO_3$ and $BiGaO_3$, our results agree well with those calculated using different methods and/or lattice constants.[13] It can be seen that both Bi and O2

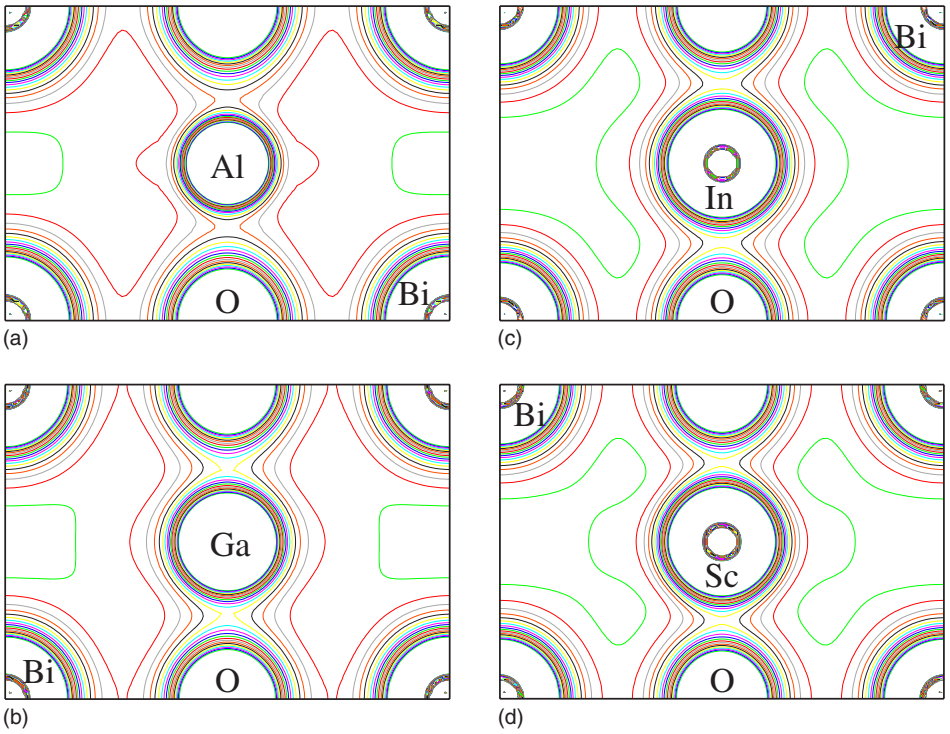

FIG. 3. (Color online) Charge density maps for cubic BiMO_3 in (110) plane.

ions have much larger effective charges, while the values for the M ions are not much different from their nominal ionic charges. The electron transfer is seen to take place in different ways, because Al and In partially capture charges while Ga and Sc lose electrons. Thus, the charge transfer in $BiAlO_3$ and $BiInO_3$ is from Bi to M (Al, In) and O ions, while that in $BiGaO_3$ and $BiScO_3$ is from Bi and M (Ga, Sc) to O ions. This different behavior of the M ions may be the cause of the structure difference.

It has been suggested that there is a strong correlation between $Z^*(A)$ and $Z^*(O2)$, as well as $Z^*(B)$ and $Z^*(O1)$ in titanate with a formula of ABO_3.[40] A similar correlation is also observed in the four BiMO_3 compounds. The values of $Z^*(Bi)$ and $Z^*(O2)$ increase according to the order Al-Ga-Sc-In, while those of $Z^*(M)$ and $Z^*(O1)$ increase according to the orders In-Al-Ga-Sc and Al-In-Sc-Ga, respectively. Also, as shown in Ref. 40, the values of $\Delta=|Z^*(O1)-Z^*(O2)|$ are about 3.5, 2.5, and 5.3 for titanate, zirconate, and niobate, respectively, whereas for BiMO_3, Δ has a value as small as $1.2|e|$ for $M=$In or even $0.08|e|$ for $M=$Sc. This suggests a strong interaction between $M-$O1 and Bi–O2 bonds and a predominant role played by the M ions in the structural instability of the BiMO_3 compounds. This is consistent with our analysis of electronic properties in Sec. III B, i.e., the $M-$O bonding dictates the details of Bi-O hybridization. Thus, the bonding character of BiMO_3 should be different from those of the titanates including $PbTiO_3$. This suggests that the four BiMO_3 actually belong to a new type of materials and the BEC is a useful property to describe the local bonding. It is well known that the large BEC of ions is related to the large displacement associated with the ferroelectric instability.[8] Consequently, the displacements of the Bi and O2 ions are probably what induce the ferroelectric phase transition. The origin of ferroelectricity will be re-examined in detailed in a later section.

TABLE III. Born effective charges and dielectric constant ϵ_∞ of four cubic BiMO_3 compounds.

	$BiAlO_3$	$BiGaO_3$	$BiInO_3$	$BiScO_3$
Bi	6.41	6.47	6.83	6.58
	6.22[a]	6.29[a]		
M	2.80	3.05	2.72	3.75
	2.84[a]	3.11[a]		
O1[b]	−2.32	−2.54	−2.38	−3.41
	−2.34[a]	−2.58[a]		
O2	−3.47	−3.52	−3.58	−3.53
	−3.38[a]	−3.40[a]		
|O1-O2|	1.15	0.98	1.20	0.08
ϵ	8.41	9.01	10.88	10.87

[a]From Ref. 13.

[b]O1 denotes the oxygen atom in the direction of B-O bond, while O2 means the one in the perpendicular direction.

We note that the optical dielectric constants ϵ_∞ of the four BiMO_3 are substantially larger than those of cubic titanates such as $BaTiO_3$, $PbTiO_3$, and $PbZrO_3$. The corresponding theoretical values are 6.75, 8.24, and 6.97, respectively. It is reasonable to expect that BiMO_3 may be promising dielectric materials. Due to the strong covalent bonding and the anomalously large BECs, BiMO_3 should also be promising ferroelectric and piezoelectric candidates for lead-free applications.

2. Zone-center phonon modes

According to the soft-mode theory, ferroelectric phases may be related to the high-temperature high-symmetric

TABLE IV. Zone-center phonon modes (cm^{-1}) and eigenvectors of four cubic $BiMO_3$ compounds. For $BiInO_3$, $O1_{BI}=(0.0,0.6108,0.1153)$, $O2_{BI}=(-0.3538,0.0,-0.1153)$, and $O3_{BI}=(0.3538,-0.6108,0.0)$. For $BiScO_3$, $O1_{BS}=(0.0,0.6108,0.1153)$, $O2_{BS}=(-0.3538,0.0,-0.1153)$, and $O3_{BS}=(0.3538,-0.6108,0.0)$.

	Mode	Soft mode	Eigenvector (Bi, *M*, O1, O2)
$BiAlO_3$	TO	−166	(−0.1506, 0.2470, 0.3656, 0.5922)
$BiGaO_3$	TO	−158	(−0.1875, 0.1999, 0.3528, 0.6125)
$BiInO_3$	TO	−262	(−0.1204, 0.0272, 0.1208, 0.6286)
		−229	(0.0, 0.0, $O1_{BI}$, $O2_{BI}$, $O3_{BI}$)
$BiScO_3$	TO	−233	(−0.1415, 0.0945, 0.2327, 0.6752)
		−195	(0.0, 0.0, $O1_{BS}$, $O2_{BS}$, $O3_{BS}$)

structure by the freezing in of unstable zone-center phonons. Indeed, zone-center phonon modes are useful properties to study to gain some insight into the physics of ferroelectric instability. The zone-center phonon modes are computed for the cubic $BiMO_3$ using DFPT and are summarized in Table IV, only giving the soft modes and their eigenvectors. $BiAlO_3$ and $BiGaO_3$ compounds have one soft mode, while $BiInO_3$ and $BiScO_3$ have 2. The first soft mode, a transverse optical (TO) phonon, corresponds to the motion of Bi ion opposite to the other ions. The value of eigenvector of O2 is largest. The *M* ions basically have no effect on the displacements of Bi and O ions. From the point of view of lattice dynamics theory, the structural instability (ferroelectricity) of $BiMO_3$ comes from the Bi and O ions. Both $BiInO_3$ and $BiScO_3$ have two soft modes; this is consistent with the fact that the two compounds have low-symmetry ground structures. Up to this point, nevertheless, we have no definitive evidence for the absence of ferroelectricity in $BiGaO_3$, although the *M* ion (Ga) is only one of the key factors.

D. Structural instability and its driving force

To explain the absence of ferroelectricity in $BiGaO_3$, we now examine the structural instability and its driving force using the PES method. The PESs are obtained by displacing each ion keeping the rest of the ions frozen. The details of the calculations can be found elsewhere.[25–28] Figure 4 shows the PES of ions along the tetragonal [001] and rhombohedral [111] directions in $BiAlO_3$ and $BiGaO_3$ at their predicted equilibrium lattice constant and 1% volume expansion. We performed the calculations assuming 1% volume expansion to examine the volume dependence of the structural instability, which is very important for titanate. In both compounds, energy reduction can only be accomplished with the off-center displacement of the Bi ion, indicating that the driving force of structural instability only comes from Bi ion. Due to the symmetry of cubic structure, all the PESs of Bi ions along the ⟨100⟩ crystallographic direction families are equivalent with multiplicity of 6, i.e., there are six [100] minima. Similarly, there are 12 [110] and 8 [111] minima which are equivalent. From Fig. 4, it is observable that the eight [111] minima are the smallest among all minima ([110] minima are not given). It is interesting to note that the eight

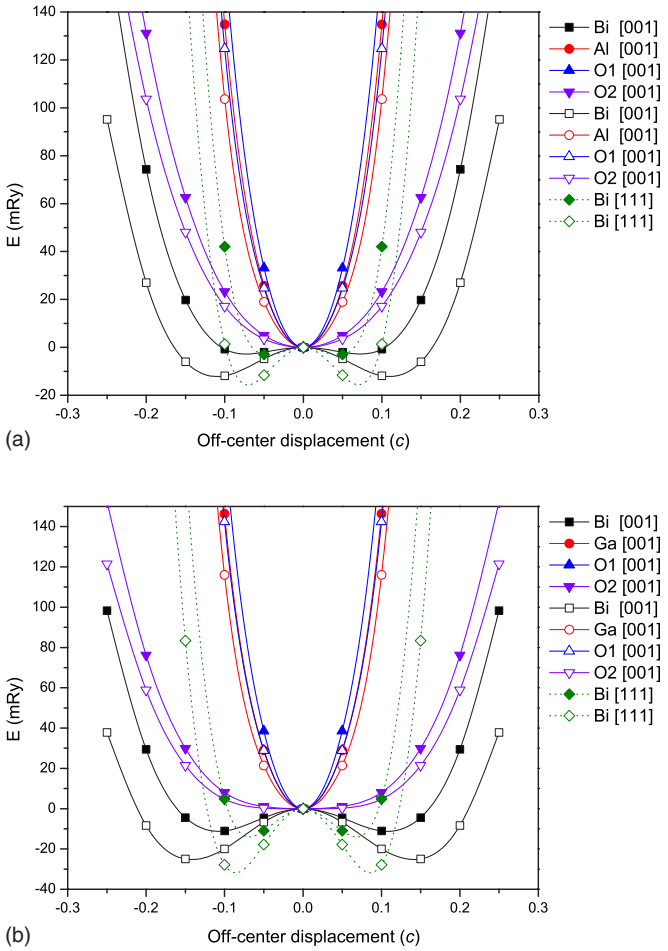

FIG. 4. (Color online) Profiles of PES for the displacement of ions along the tetragonal [001] (lines) and rhombohedral [111] (dot lines) in cubic $BiAlO_3$ (up) and $BiGaO_3$ (down) at predicted equilibrium lattice constant and 1% volume expansion indicated by solid and vacuity symbols, respectively.

[111] minima obtained by the PES method are consistent with eight-site model,[41] based on which the order-disorder character of the phase transition in $BaTiO_3$ has been successfully explained.[42] The same reasoning can be used to confirm the order-disorder character of the phase transition for the materials considered here. Like Ti ions in $BaTiO_3$, Bi ions in $BiMO_3$ have eight minima and occupied one of the eight off-center positions in the cubic unit cell along the ⟨111⟩ directions. Following the model of Blinc and co-workers for $BaTiO_3$,[42,43] the phase transition of $BiAlO_3$, consequently, can also be readily understood. The cubic phase consists of random distortions along eight cube diagonals [111], and the tetragonal phase consists of displacements along four cube diagonals giving an average structure with a polarization along [001], while the rhombohedral phase is ordered along [111]. In addition, the PES of the O2 ions is very close to that of Bi, suggesting a coupling between anion O2 and Bi ions, indicating a contribution to the instability. Following Ref. 28, both $BiAlO_3$ and $BiGaO_3$ are *A*-site driven ferroelectrics like $PbZrO_3$, and its instability comes from the Bi^{3+} ion, suggesting that the PES is a valuable tool for exploring the driving force of structural instability. Similarly, the struc-

tural instability in titanate such as $BaTiO_3$ comes from *B*-site cation Ti.[28]

The [110] in-plane instability is larger in $BiGaO_3$ than in $BiAlO_3$. In $BiGaO_3$, the large instability due to in-plane rotation makes it an orthorhombic structure, while in $BiAlO_3$, the much smaller instability due to in-plane rotation results in a rhombohedral structure. It is observable that volume expansion enhances both tetragonal and rhombohedral instabilities as well as the in-plane instability (Fig. 4), similar to that of $BaTiO_3$.[44] The potential energy surfaces indicate that the driving force of the structural instability (ferroelectricity) in BiMO_3 comes from the $6s^2$ lone pair of Bi ion, while the density of states, Born effective charges, and soft-mode eigenvectors suggest that the structural instability is associated with the Bi and O ions, i.e., Bi-O hybridization is essential for ferroelectricity in the BiMO_3 compounds. As mentioned in the foregoing, BECs also suggest that there is a strong interaction between M-O1 and Bi-O2 bonds, and the *M* ions may have a dominant role in the structural instability of BiMO_3. We conjecture that the partial charges gained by the Al ions will enhance the Bi-O coupling, while the partial charges lost by the Ga ion increases the interaction between Ga-O1 and Bi-O2. At the same time, the interaction of Ga-O1 will reduce the coupling of Bi-O2. In this context, it is not surprising that the $BiGaO_3$ is not ferroelectric and BiMO_3 compounds (M=Al, Ga, In, and Sc) possess different structures at room temperature.

IV. CONCLUSIONS

In summary, we have performed first-principles density-functional calculations to systematically investigate the structural and electronic properties of compounds of the type BiMO_3, where *M* stands for a metallic ion. In this paper, we consider three IIIB-group metals (M=Al, Ga, and In) and one IIIA transition metal (M=Sc). Optimized lattice parameters, bulk moduli, band structures, densities of states, and charge density distributions are obtained. Our results are in good agreement with other calculations in the literature. We found that their electronic properties vary with *M* through their effects on the Bi-O bonding. This points to the possibility that the properties of BiMO_3 may be tuned according to design by appropriately choosing the *M* ion and/or combination of different *M* ions. For example, the band gap between the occupied O $2p$ and unoccupied Bi $6p$ sates can be changed between the wide range from 0.17 to 1.57 eV by varying the *M* ion.

Similar to the titanates, BiMO_3 have anomalously large Born effective charges, despite the *B*-site *M* ions that are very close to their formal ionic values. The BECs also show strong interrelations between the *M*-O1 and Bi-O2 bonds, which are not strong in titanate, zirconate, and niobate, indicating that the *M* ions have a dominant role in the structural instability of the BiMO_3. The driving force of structural instability (ferroelectricity) is found to be from the $6s^2$ lone pair on the *A*-site Bi ion, while the calculated Born effective charges and soft-mode eigenvectors suggest that the structural instability is related to both the Bi and O ions. Consequently, the structural transition in BiMO_3 may occur in the following sequence: First, the Bi ion is displaced off center to one of the eight [111] minima, coupling with the anion O. This induces a cooperative movement of ions in the crystal and results in the phase transforming of the cubic crystal system to a lower-symmetry structure. As a result, the *M* ions play a determining role in the transformation. Thus, for example, the nonferroelectric nature of the transformation of $BiGaO_3$ is due to the dominant in-plane structural instability caused by Ga. Considering the soft modes and eight [111] minima, we suggest that the phase transition in BiMO_3 should have a mixed displacive and order-disorder character. In terms of PES of ions, BiMO_3 compounds are *A*-site driven ferroelectrics, the properties of which can be tuned by the introducing a proper *M* ion. This may be the key to the understanding of the variability of properties of BiMO_3 with distinct structures and to the physics of *tunable* ferroelectrics. In addition, BiMO_3 are found to have relatively larger optical dielectric constants than other perovskite and should therefore be promising dielectric materials. BiMO_3 or its derivatives are thus interesting as ferroelectric, piezoelectric, multiferroic, and photocatalytic materials.

ACKNOWLEDGMENTS

This project was supported by the National Natural Science Foundation of China (10572155 and 10172030) and the Foundation of Guangdong Province (2005A10602002).

[1] R. E. Eitel, C. A. Randall, T. R. Shrout, P. W. Rehrig, W. Hackenberger, and S.-E. Park, Jpn. J. Appl. Phys., Part 1 **40**, 5999 (2001).
[2] R. E. Eitel, C. A. Randall, T. R. Shrout, and S.-E. Park, Jpn. J. Appl. Phys., Part 1 **41**, 2099 (2002).
[3] S. J. Zhang, C. A. Randall, and T. R. Shrout, Appl. Phys. Lett. **83**, 3150 (2003).
[4] J. R. Cheng, W. Y. Zhu, N. Li, and L. E. Cross, Mater. Lett. **57**, 2090 (2003).
[5] R. R. Duan, R. F. Speyer, E. Alberta, and T. R. Shrout, J. Mater. Res. **19**, 2185 (2004).
[6] Y. Inaguma, A. Miyaguchi, M. Yoshida, T. Katsumata, Y. Shimojo, R. P. Wang, and T. Sekiya, J. Appl. Phys. **95**, 231 (2004).
[7] S. J. Zhang, R. Xia, C. A. Randall, T. R. Shrout, R. R. Duan, and R. F. Speyer, J. Mater. Res. **20**, 2067 (2005).
[8] J. Iniguez, D. Vanderbilt, and L. Bellaiche, Phys. Rev. B **67**, 224107 (2003).
[9] N. A. Hill and K. M. Rabe, Phys. Rev. B **59**, 8759 (1999).
[10] R. Seshadri and N. A. Hill, Chem. Mater. **13**, 2892 (2001).
[11] T. Atou, H. Chiba, K. Ohoyama, Y. Yamaguchi, and Y. Syono, J. Solid State Chem. **145**, 639 (1999).
[12] A. Moreira dos Santos, A. K. Cheetham, T. Atou, Y. Syono, Y. Yamaguchi, K. Ohoyama, H. Chiba, and C. N. R. Rao, Phys. Rev. B **66**, 064425 (2002).

[13] P. Baettig, C. F. Schelle, R. LeSar, U. V. Waghmare, and N. A. Spaldin, Chem. Mater. **17**, 1376 (2005).
[14] A. A. Belik, M. Takano, M. V. Boguslavsky, S. Y. Stefanovich, and B. I. Lazoryak, Chem. Mater. **18**, 133 (2006).
[15] A. A. Belik, S. Y. Stefanovich, B. I. Lazoryak, and E. Takayama-Muromachi, Chem. Mater. **18**, 1964 (2006).
[16] A. A. Belik, S. Iikubo, K. Kodama, N. Igawa, S. Shamoto, M. Maie, T. Nagai, Y. Matsui, S. Y. Stefanovich, B. I. Lazoryak, and E. Takayama-Muromachi, J. Am. Chem. Soc. **128**, 706 (2006).
[17] N. A. Hill, J. Phys. Chem. B **104**, 6694 (2000).
[18] N. A. Hill, Annu. Rev. Mater. Res. **32**, 1 (2002).
[19] M. Fiebig, J. Phys. D **38**, R123 (2005).
[20] W. Prellier, M. P. Singh, and P. Murugavel, J. Phys.: Condens. Matter **17**, R803 (2005).
[21] R. D. King-Smith and D. Vanderbilt, Phys. Rev. B **49**, 5828 (1994).
[22] E. Mete, R. Shaltaf, and S. Ellialtioglu, Phys. Rev. B **68**, 035119 (2003).
[23] J. Junquera and P. Ghosez, Nature (London) **422**, 506 (2003).
[24] K. Johnston, X. Y. Huang, J. B. Neaton, and K. M. Rabe, Phys. Rev. B **71**, 100103(R) (2005).
[25] R. E. Cohen, Nature (London) **358**, 136 (1992).
[26] Z. X. Chen, Y. Chen, and Y. S. Jiang, J. Phys. Chem. B **105**, 5766 (2001).
[27] Z. X. Chen, Y. Chen, and Y. S. Jiang, J. Phys. Chem. B **106**, 9986 (2002).
[28] M. Ghita, M. Fornari, D. J. Singh, and S. V. Halilov, Phys. Rev. B **72**, 054114 (2005).
[29] H. Wang, B. Wang, R. Wang, and Q. K. Li, Physica B **390**, 96 (2007).
[30] P. Blaha, K. Schwarz, G. K. H. Madsen, D. Kvasnicka, and J. Luitz, WIEN2K, an augmented plane wave plus local orbitals program for calculating crystal properties, Vienna University of Technology, Vienna, 2001.
[31] J. P. Perdew and Y. Wang, Phys. Rev. B **45**, 13244 (1992).
[32] J. P. Perdew, K. Burke, and M. Ernzerhof, Phys. Rev. Lett. **77**, 3865 (1996).
[33] S. Baroni, A. Dal Corso, S. de Gironcoli, P. Giannozzi, C. Cavazzoni, G. Ballabio, S. Scandolo, G. Chiarotti, P. Focher, A. Pasquarello, K. Laasonen, A. Trave, R. Car, N. Marzari, and A. Kokalj, http://www.pwscf.org/
[34] P. Hohenberg and W. Kohn, Phys. Rev. **136**, B864 (1964).
[35] W. Kohn and L. Sham, Phys. Rev. **140**, A1133 (1965).
[36] S. Baroni, S. Gironcoli, and A. D. Corso, Rev. Mod. Phys. **73**, 515 (2001).
[37] F. D. Murnaghan, Proc. Natl. Acad. Sci. U.S.A. **30**, 5390 (1944).
[38] A. Dal Corso, A. Pasquarello, A. Baldereschi, and R. Car, Phys. Rev. B **53**, 1180 (1996).
[39] P. E. Blochl, O. Jepsen, and O. K. Andersen, Phys. Rev. B **49**, 16223 (1994).
[40] W. Zhong, R. D. King-Smith, and D. Vanderbilt, Phys. Rev. Lett. **72**, 3618 (1994).
[41] R. Cornes, M. Lambert, and A. Guinier, Acta Crystallogr., Sect. A: Cryst. Phys., Diffr., Theor. Gen. Crystallogr. **A26**, 244 (1970).
[42] R. Pirc and R. Blinc, Phys. Rev. B **70**, 134107 (2004).
[43] B. Zalar, V. V. Laguta, and R. Blinc, Phys. Rev. Lett. **90**, 037601 (2003).
[44] R. E. Cohen and H. Krakauer, Phys. Rev. B **42**, 6416 (1990).